**HEAT TRANSFER**

https://onlinelibrary.wiley.com/journal/26884542

*Editor-in-chief: Prof. William M. Worek, Texas, USA.*

*Online ISSN:2688-4542*

**Accepted November 24th 2021**

# UNSTEADY MAGNETOHYDRODYNAMIC COUPLE STRESS FLUID FLOW FROM A SHRINKING POROUS SHEET: VARIATIONAL ITERATION METHOD STUDY

**G. Janardhana Reddy[1, *], Ashwini Hiremath[1], Mahesh Kumar[2], O. Anwar Bég[3] and Ali Kadir[3]**

[1]*Department of Mathematics, Central University of Karnataka, Kalaburagi,* ***India.***

[2]*Department of Mathematics and Humanities, Sardar Vallabhbhai National Institute of Technology, Surat, Gujarat-395007, India.*

[3]*Aeronautical/Mechanical Engineering, SEE, University of Salford, Manchester M54WT,* ***UK.***

[*]***Corresponding author - Email:*** **gjr@cuk.ac.in**

**ABSTRACT:** Motivated by magnetic polymer manufacturing applications, the present research article examines theoretically the hydromagnetic boundary layer flow of an electrically conducting non-Newtonian couple stress fluid due to a transient shrinking (contracting) porous sheet. The conservation partial differential equations for mass and momentum are rendered into a fifth order non-linear ordinary differential equation via similarity transformations with associated boundary conditions. A semi-analytical/numerical scheme employing Lagrangian multipliers and known as the variational iteration method (VIM) is implemented to solve the ordinary differential boundary value problem. Validation of the solutions is conducted by benchmarking against earlier Newtonian studies and very good agreement is achieved. A detailed assessment of the impact of couple stress (rheological), unsteadiness, magnetic body force parameter and wall transpiration (suction/injection) parameter on flow characteristics is conducted with the aid of graphs. Significant deceleration in the flow is computed with increasing injection (acceleration is caused with greater suction) and acceleration is induced with higher unsteadiness parameter values. Increasing magnetic field (higher magnetic number) generates flow acceleration, rather than the customary deceleration, due to the shrinking sheet dynamics. Stronger couple stress effect manifests in a strong retardation in the boundary layer flow and an increase in momentum (hydrodynamic|) boundary layer thickness. VIM demonstrates excellent convergence and accuracy and shows significant promise in studying further magnetic polymer fabrication flow problems.

**KEYWORDS:** *Shrinking sheet; couple stress rheological liquid; MHD; polymer processing, VIM; Unsteadiness.*

## 1. INTRODUCTION

The laminar boundary layer flow from a shrinking sheet geometry is an important type of flow arising in chemical engineering, packaging processes and the manufacturing of polymer sheets. It is somewhat dissimilar from the stretching sheet flow and the physical configuration of shrinking flow is quite complex. This method offers certain advantages in terms of stability of thin film packaging techniques, uniformity of the enrobing, tightness of fitting and cost-effectiveness. The majority of packaging films used for shrink-wrapping (and coating) are from the polyolefin range and derived from oil-based chemicals via a polymerization process (polyethylene, polypropylene and poly vinyl chloride) [1]. In shrinking sheet flows, the sheet movement is in the opposite direction to that of the stretching case, and thus the flow occurs towards a slot. Since such flows are viscous and controlled largely by wall (boundary) conditions, a powerful framework for their simulation is the use of *boundary layer* models. Once the velocity field has been computed, coating thickness and other characteristics can be evaluated [2]. Wang [3] first analyzed the shrinking sheet flow problem. Miklavcˇicˇ and Wang [4] subsequently extended the analysis in [3] to study the suction effect at the wall for the case of a porous sheet, noting that within the boundary layer the vorticity of the shrinking sheet is not restrained, and the fluid flow is improbable to occur unless sufficient suction on the boundary is achieved. Building on these earlier investigations, considerable interest has been mobilized in analyzing shrinking sheet flows, for both unsteady and steady-state conditions. The sheet may be stretched with linear, quadratic or exponential velocity [5,6]. Ali *et al*. [7] studied the time-dependent fluid flow problem for shrinking sheet using the Keller-box finite difference computational scheme. Prasad *et al.* [8] considered the heat transfer flow for non-linear porous shrinking sheet. Hafidzuddin *et al.* [9] presented the 3D viscous flow for a permeable shrinking sheet. Ghosh *et al.* [10] examined the slip flow from a non-linearly permeable shrinking sheet. Uddin and Bhattacharyya [11] analyzed the thermal boundary layer flow from a non-isothermal permeable shrinking sheet.

These investigations were confined to Newtonian fluids. Polymers are inherently non-Newtonian [12] and exhibit diverse material characteristics including viscoplasticity, shear-thinning, shear-thickening, viscoelasticity, rheopetic behavior etc [13, 14]. Several researchers have simulated shrinking sheet flows with a variety of rheological models. Zaib *et al*. [15] used a viscoplastic Casson model to derived dual solutions for convection dissipative flow from an exponentially

permeable shrinking sheet. Mehmood *et al*. [16] used a Reynolds exponential viscosity model and successive linearization technique to compute the shrinking rate effects on non-orthogonal contracting sheet stagnation flow with applications in solar nano-surfacing systems. Other models employed include the Ostwald-deWaele power-law model [17, 18], Eringen micropolar model [19, 20], Casson model [21]. Naganthrana *et al.* [23] studied the non-Newtonian viscoelastic fluid flow from a shrinking surface with a finite difference scheme. Gupta *et al.* [24] used a variational finite element code to study the micropolar flow from a radially shrinking sheet with convective wall cooling and radiative flux effects. Mishra *et al.* [24] analyzed the micropolar convection flow from a shrinking sheet with heat generation effects. Khan *et al.* [25] used a Runge–Kutta Fehlberg shooting method to compute the Carreau fluid flow problem from a shrinking surface with infinite shear rate viscosity. Latiff *et al.* [26] used MAPLE quadrature and a modified micropolar rheological model to investigate the time-dependent slip flow, heat and species diffusion from nanoparticle and micro-organism-doped polymeric stretching/shrinking sheets. With the exception of the micropolar fluid, the other non-Newtonian constitutive models neglect micro-structural characteristics of the liquid. Polymers contain suspensions which dramatically modify their internal constitution and particles (micro-elements) may spin and deform. To accurately model polymer flows therefore, the simpler non-Newtonian models and Navier-Stokes Newtonian models are clearly inadequate. A simpler framework than micropolar models [19, 20, 26] is provided by Stokes couple stress ("polar") model [27, 28]. This neglects micro-rotation characteristics but includes couple stresses. It effectively produces a higher order to the momentum equations due to the polar (couple stress) contribution. The couple stress model has been successively deployed to simulate a variety of complex rheological flows including polymers, lubricants, blood, squeezing film flow, electro-osmotic [29] and magneto-rheological smart fluids [30] and also supercritical thermodynamic coating systems [31]. These studies have confirmed that couple stresses significantly modify momentum diffusion, bulk flow and boundary layer-characteristics and that their neglection leads to erroneous estimates of flow behavior. Comprehensive details on the hydrodynamics of couple stress fluids are available in Stokes [28].

Electro-conductive (magnetic) polymer has emerged in recent years as an exciting and novel branch of magnetic materials; it combines the metal properties such as electrical conductivity with non-Newtonian characteristics of polymers [32, 33]. Such materials have applications in smart coating systems [34] which are frequently deployed via shrinking sheet dynamics in industrial

fabrication assemble line systems. To increase the production of these magnetic polymers, a mathematical model is needed which combines the magnetohydrodynamics (MHD) properties and theoretical rheology. Also, the powerful numerical technique for the solution system of equations. The practice of these advance leveled multi-physical fluid dynamics models can considerably optimize the synthesis processes for such materials and contributes in enhancement of the quality control. The manipulation in the performance and structure of the polymer can be done with the sensible use of an *applied magnetic field* and control over the flow instabilities and homogeneity in products can be achieved. In the most common magnetic materials processing operation a transverse static uniform magnetic field is employed to generate the Lorentz body force which can accelerate/decelerate flows in the boundary layer [32]. However other phenomena may arise including Hall currents, Joule magnetic dissipation, oblique magnetic field, alternating fields, magnetic flux leakage etc. Many investigators have simulated magnetic non-Newtonian flows from shrinking sheets (contractional) by extending the original Newtonian magnetohydrodynamic model of Pavlov [25]. Bég *et al.* [36] used finite difference and spectral methods to compute the shrinking and magnetic field effects on rheological nano-magnetic polymer flow over a contracting surface. Thumma *et al.* [37] employed a high penalty (hp) finite element method and Buongiorno's nanoscale model to evaluate the influential action of viscous heating, heat generation and absorption on power-law stretching or shrinking sheet flow of a magnetic nanopolymer. Further studies include Cortell [38], Noor *et al.* [39], Merkin and Kumaran [40], Zheng *et al.* [41] although these were restricted to Newtonian magnetic shrinking sheet flows. Non-Newtonian magnetohydrodynamic shrinking sheet flows have also been studied by Hayat *et al.* [42] (using the Reiner-Rivlin viscoelastic model) and Uddin *et al.* [43] (using power-law nanofluid models). All these studies have demonstrated the significant influence of magnetic field on fluid dynamic characteristics in shrinking sheet systems.

As noted earlier, the nonlinear nature of boundary value problems describing rheological magnetic polymer shrinking sheet flows generally requires very powerful and efficient semi-analytical/analytical and numerical schemes for solving the nonlinear differential equations. Many versatile numerical and analytical methods have therefore emerged including grid point techniques, perturbation, homotopy, cubic spline, differential transform, Adomian, generalized differential quadrature and spectral techniques. Each of these techniques however has one or more limitations. The variational iteration method (VIM) was developed by He [44] and is a relatively

simple and easy semi-analytical method for differential equations. VIM yields fast convergent approximations to the exact solution without restrictions or unrealistic assumptions. VIM is a kind of Lagrange multiplier method and involves building correction functionals for given problems via variational theory. The applications of VIM are found in solving Lotka–Volterra equations [45], hydromagnetic flows [46, 47], flow over a moving belt [48], non-Newtonian reactive thermal duct propulsion flows [49] and bio-thermal physics [50]. VIM and its applications in magnetic materials processing are reviewed in detail in Bég [51].

Inspection of the literature has shown that thus far VIM has not been applied to simulate the unsteady magnetohydrodynamic couple stress shrinking porous sheet flow. Consequently, the main aim of this study is to analyze the transient hydromagnetic couple stress fluid from a shrinking sheet with VIM under transverse *unsteady* magnetic field. Suction and injection effects are simulated at the sheet (wall). The research article is organized as follows: Section 1 is the introduction with literature review. Section 2 entails the formulation of the problem. Extensive details of the solution by VIM is discussed in Section 3. The graphical and tabulated results and discussion are presented in Section 4. Succinct conclusions and recommendations for future work are elaborated in Section 5.

## 2. MATHEMATICAL FORMULATION

Consider the unsteady, two-dimensional, laminar boundary layer flow of an incompressible couple stress fluid bounded by a porous shrinking sheet is considered and portrayed in **Fig. 1**. The considered fluid is electrically conducting under the effect of normally applied transient magnetic field $B(t)$. The chosen $x$-coordinate runs parallel to the surface and $y$-coordinate is perpendicular to it. Electron pressure is negligible and magnetic field is weak enough to negate Hall current, ion slip and electromagnetic induction effects. The governing flow-field equations for couple stress fluid with unsteadiness can be written as follows:

$$\frac{\partial u}{\partial x}+\frac{\partial v}{\partial y}=0 \tag{1}$$

$$\rho\left(\frac{\partial u}{\partial t}+u\frac{\partial u}{\partial x}+v\frac{\partial u}{\partial y}\right)= \mu\frac{\partial^2 u}{\partial y^2}-\eta_1\frac{\partial^4 u}{\partial y^4}-\sigma B^2(t)u \tag{2}$$

For transient shrinking sheet, the boundary conditions are defined at the wall and in the free stream as follows:

$$u = U_w\ ,\ \frac{\partial^2 u}{\partial y^2} = 0\ ,\ v = V_w \qquad \text{at}\ \ y = 0$$

$$u \to 0 \quad \text{and} \quad \frac{\partial u}{\partial y} \to 0 \qquad \text{as}\ \ y \to \infty \tag{3}$$

where $u$ and $v$ are the velocity components in $x$, $y$ coordinates, $\rho$ is the density of the couple stress fluid, $\mu$ is the dynamics viscosity, $\eta_1$ couple stress fluid viscosity and $\sigma$ is the electric conductivity.

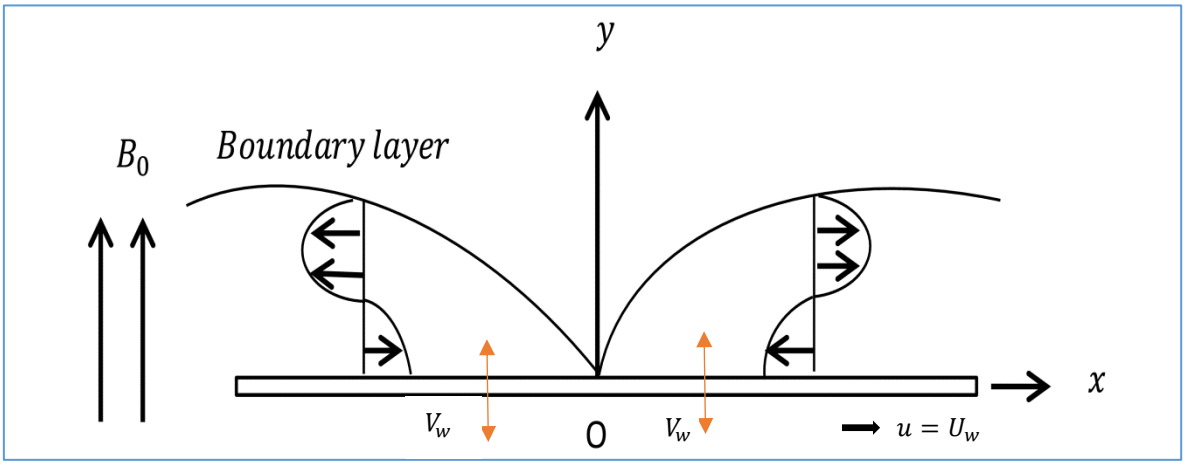


**Fig. 1:** Schematic of shrinking sheet flow of a magnetic couple stress fluid.

Further the sheet shrinking velocity $U_w(x,t)$, porous wall transpiration (lateral mass flux) velocity $V_w(x,t)$ and unsteady magnetic field $B(t)$ are of the form:

$$U_w(x,t) = -\frac{U_0 x}{(1-at)} \quad \text{and} \quad V_w(x,t) = -f(0)\sqrt{\frac{\nu U_0}{(1-at)}}, \tag{4a}$$

$$B(t) = \frac{B_0}{(1-at)} \tag{4b}$$

Where $U_0$ is constant, $a$ represents unsteadiness of the problem and $B_0$ is denotes applied magnetic field, and both have a dimension of frequency (inverse of time). Further, when $t = 0$, the partial differential Eqns. (1)-(2) represents the time-dependent flow of a couple stress fluid from a shrinking sheet. These specific forms of $U_w$ , $V_w$ and $B(t)$ have been formulated in order to derive a new similarity transformation, which renders the governing non-linear *partial* differential

equations (1)-(2) into a set of non-linear *ordinary* differential equations. Introducing the dimensionless function $f$ and similarity variable $\eta$ (transformed transverse coordinate) as follows [52, 53]:

$$\eta = \sqrt{\frac{U_0}{\upsilon(1-at)}}\, y\,,\ \psi = \sqrt{\frac{U_0 \upsilon}{(1-at)}}\, x f(\eta) \tag{5}$$

Here $\psi(x, y, t)$ is the stream function such that $u = \frac{\partial \psi}{\partial y}$ , $v = -\frac{\partial \psi}{\partial x}$ which satisfies Eqn. (1) i.e., equation of continuity. Introducing Eqn. (5) into Eqns. (1) and (2) yields:

$$\xi f^{v} - f''' + f'^{2} - f f'' + \frac{1}{2}\beta \eta f'' + (M^2 + \beta) f' = 0 \tag{6}$$

Here prime represents differentiation with respect to $\eta$, $\xi = U_0 \eta_1 / \upsilon^2 \rho (1 - at)$ is the couple stress (rheological) parameter, $\beta = a/U_0$ is the unsteadiness parameter, $M^2 = \sigma B_0^2 / \rho U_0 (1 - at)$ is the square of the magnetohydrodynamic body force number.

The associate boundary conditions are:

$$f(0) = \alpha, f'(0) = -1, f'''(0) = 0 \quad \text{at } \eta = 0$$

$$f'(\eta) \to 0,\ f''(\eta) \to 0 \qquad \text{as } \eta \to \infty \tag{7}$$

Here α is the wall transpiration velocity (for suction, $\alpha > 0$ and for injection $\alpha < 0$). The local skin-friction coefficient $C_f$ is a key design parameter in materials processing systems (it provides a measure of the drag on the wall due to the surface shear stress) and is defined as:

$$C_f = \frac{\tau_w}{\rho {U_w}^2 / 2}, \tag{8a}$$

The wall skin-friction (dimensional shear stress) $\tau_w$ is defined as;

$$\tau_w = \mu \left(\frac{\partial u}{\partial y}\right)_{y=0} \quad \text{then} \quad \frac{1}{2} C_f Re^{1/2} = f''(0) \tag{8b}$$

Here *Re* is Reynolds number.

## 3. VIM SOLUTION OF BOUNDARY VALUE PROBLEM

The variational iteration method (VIM) has been implemented to solve the transformed nonlinear fifth-order ordinary differential momentum Eqn. (6) with boundary conditions (7). To represent the fundamental idea of the variational iteration technique, the following general nonlinear system is taken into consideration [44, 46-51]:

$$\mathcal{L}[u(x)] + \aleph[u(x)] = \mathcal{F}(x) \tag{9}$$

where $\mathcal{L}$ denotes a linear operator, $\aleph$ is a nonlinear operator, and $\mathcal{F}(x)$ represents continuous function. A key feature of VIM is to make a *correctional function* for a given system of equations as follows:

$$u_{n+1}(x) = u_n(x) + \int_{x_0}^{x} \lambda(s)\{\mathcal{L}u_n(s) + \aleph\tilde{u}_n(s) - \mathcal{F}(s)\}\, ds \tag{10}$$

where $\lambda(s)$ denotes a usual Lagrange multiplier which could be ascertained optimally through variational theory, $u_n$ is the solution of the n[th] approximation, and $\tilde{u}_n$ signifies a restricted variation, i.e., $\delta\tilde{u}_n$.

Now, according to VIM Eqn. (6) can be expressed as:

$$f_{n+1}(\eta) = f_n(\eta) + \int_0^{\eta} \lambda(s) \left[ \frac{\partial^5 f_n(s)}{\partial s^5} - \frac{1}{\xi} \begin{pmatrix} \frac{\partial^3 f_n(s)}{\partial s^3} - \left(\frac{\partial \tilde{f}_n(s)}{\partial s}\right)^2 + \tilde{f}_n(s) \frac{\partial^2 \tilde{f}_n(s)}{\partial s^2} \\ -\frac{1}{2}\beta\eta \frac{\partial^2 f_n(s)}{\partial s^2} - (M^2 + \beta) \frac{\partial f_n(s)}{\partial s} \end{pmatrix} \right] ds \tag{11}$$

Taking variation with respect to the variable $\tilde{f}(s)\frac{\partial^2 \tilde{f}(s)}{\partial s^2}$ and $\left(\frac{\partial \tilde{f}(s)}{\partial s}\right)^2$ and noticing that $\delta\tilde{f}(s)\frac{\partial^2 \tilde{f}(s)}{\partial s^2} = 0$ and $\delta\left(\frac{\partial \tilde{f}(s)}{\partial s}\right)^2 = 0$, then Eqn. (11) implies:

$$\delta f_{n+1}(\eta) = \delta f_n(\eta) + \delta \int_0^{\eta} \lambda(s) \left[ \frac{\partial^5 f_n(s)}{\partial s^5} - \frac{1}{\xi} \begin{pmatrix} \frac{\partial^3 f_n(s)}{\partial s^3} - \left(\frac{\partial \tilde{f}_n(s)}{\partial s}\right)^2 + \tilde{f}_n(s) \frac{\partial^2 \tilde{f}_n(s)}{\partial s^2} \\ -\frac{1}{2}\beta\eta \frac{\partial^2 f_n(s)}{\partial s^2} - (M^2 + \beta) \frac{\partial f_n(s)}{\partial s} \end{pmatrix} \right] ds \tag{12}$$

Hence, the following stationary conditions can be determined:

$$\lambda^{v}(s)|_{s=\eta} = 0$$

$$1 + \lambda^{iv}(s)\big|_{s=\eta} = 0$$

$$\vdots$$

$$\lambda'(s)|_{s=\eta} = 0$$

$$\lambda(s)|_{s=\eta} = 0 \qquad \text{(13a-c)}$$

Eventually this yields:

$$\lambda = -\frac{1}{24}(s-\eta)^4 \qquad (14)$$

Eqn. (14) can be written as:

$$f_{n+1}(\eta) = f_n(\eta) - \int_0^\eta \frac{1}{24}(s-\eta)^4 \left[ \frac{\partial^5 f_n(s)}{\partial s^5} - \frac{1}{\xi}\left( \begin{matrix} \frac{\partial^3 f_n(s)}{\partial s^3} - \left(\frac{\partial \tilde{f}_n(s)}{\partial s}\right)^2 + \tilde{f}_n(s)\frac{\partial^2 \tilde{f}_n(s)}{\partial s^2} \\ -\frac{1}{2}\beta\eta\frac{\partial^2 f_n(s)}{\partial s^2} - (M^2+\beta)\frac{\partial f_n(s)}{\partial s} \end{matrix} \right) \right] ds \qquad (15)$$

$$\forall n = 1,2, \dots \dots \dots k$$

(Eq. (15)) is coded in the **Mathematica** software and to attain reasonable accuracy, we acquire the 10-term approximation of $f(\eta)$. The first two terms are written as follows. We begin with the initial approximation:

$$f_0(\eta) = f(0) + \frac{\eta}{1!}f'(0) + \frac{\eta^2}{2!}f''(0) + \frac{\eta^3}{3!}f'''(0) + \frac{\eta^4}{4!}f^{(iv)}(0) \qquad (16)$$

Making use of initial conditions we have:

$$f_0(\eta) = \alpha - \eta + \frac{\eta^2}{2!}n_1 + \frac{\eta^4}{4!}n_2 \qquad (17)$$

where $f''(0) = n_1, f^{iv}(0) = n_2$ are to be determined using boundary conditions (7).Therefore by the above iteration formula, we obtain following series of solutions:

$$f_1(\eta) = f_0(\eta) - \int_0^\eta \frac{1}{24}(s-\eta)^4 \left[ \frac{\partial^5 f_0(s)}{\partial s^5} - \frac{1}{\xi}\left( \begin{matrix} \frac{\partial^3 f_0(s)}{\partial s^3} - \left(\frac{\partial \tilde{f}_0(s)}{\partial s}\right)^2 + \tilde{f}_0(s)\frac{\partial^2 \tilde{f}_0(s)}{\partial s^2} \\ -\frac{1}{2}\beta\eta\frac{\partial^2 f_0(s)}{\partial s^2} - (M^2+\beta)\frac{\partial f_0(s)}{\partial s} \end{matrix} \right) \right] ds$$

$$\Rightarrow f_1(\eta) = \alpha - \eta + \frac{\eta^2}{2}n_1 + \frac{\eta^4}{24}n_2 + \left(\frac{\alpha n_1}{\xi} - \frac{(1+M^2+\beta)}{\xi}\right)\frac{\eta^5}{120} + \left(\frac{n_2}{\xi} + \frac{n_1 M^2}{\xi} + \frac{n_1(2+\beta)}{2\xi}\right)\frac{\eta^6}{720}$$

$$-\left(\frac{n_1^2}{\xi} - \frac{\alpha n_2}{\xi}\right)\frac{\eta^7}{5040} - \left(\frac{n_2(2-2M^2+\beta)}{\xi}\right)\frac{\eta^8}{80640} + \cdots \qquad (18)$$

Similarly,

$$f_2(\eta) = \alpha - \eta + \frac{\eta^2}{2}n_1 + \frac{\eta^4}{24}n_2 + \left(\frac{\alpha \mathrm{n}_1}{\xi} - \frac{\left(1+M^2+\beta\right)}{\xi}\right)\frac{\eta^5}{120} + \left(\frac{\mathrm{n}_2}{\xi} + \frac{\mathrm{n}_1 M^2}{\xi} + \frac{\mathrm{n}_1(2+\beta)}{2\xi}\right)\frac{\eta^6}{720}$$

$$+ \left(\frac{-1+\alpha \mathrm{n}_1 - M^2 - \beta}{\xi^2} - \frac{\mathrm{n}_1^2}{\xi} + \frac{\alpha \mathrm{n}_2}{\xi}\right)\frac{\eta^7}{5040} - \left(\frac{2\alpha^2 \mathrm{n}_1 + 2\mathrm{n}_2 - 2\alpha\left(1+M^2+\beta\right) + \mathrm{n}_1\left(2+2M^2+\beta\right)}{\xi^2} - \frac{\mathrm{n}_2\left(2-2M^2+\beta\right)}{\xi}\right)\frac{\eta^8}{40320} + \left(\frac{\alpha\left(4\mathrm{n}_2 + \mathrm{n}_1\left(-2+4M^2-\beta\right)\right) + 2\left(2-\mathrm{n}_1^2+M^2-M^4+3\beta+\beta^2\right)}{2\xi^2} - \frac{\mathrm{n}_1 n_2}{\xi}\right)\frac{\eta^9}{362880}$$

$$+ \left(\frac{4\mathrm{n}_2(-4+\alpha^2+2M^2-2\beta) + \mathrm{n}_1(-16+4M^4-16\beta-3\beta^2-4M^2(3+\beta))}{\xi^2}\right)\frac{\eta^{10}}{14515200} +$$

$$+ \left(\frac{6\mathrm{n}_1\mathrm{n}_2 + 2\mathrm{n}_1^2(8+3M^2+4\beta) + \alpha \mathrm{n}_2(4M^2-5(2+\beta))}{\xi^2} - \frac{\mathrm{n}_2^2}{\xi}\right)\frac{\eta^{11}}{7983360} + \cdots \ldots \quad (19)$$

To evaluate above series solutions, it is necessary to obtain the unknown values of $\mathrm{n}_1$ and $\mathrm{n}_2$ , then select an appropriate numerical integration routine to determine the solution of the problem. We employ the either NSolve command or Padé method in Mathematica software [54] to get the unknown value with high accuracy. Subsequently, after substituting known values of $n_1, n_2$ into the above series solution for specific values of flow-field parameters ($M = 1.0, \alpha = 1.0, \beta = 0.2, \xi = 1.0$), the expressions of $f(\eta)$ can be written as follows:

$$f(\eta) = 1 - \eta + 0.254518\eta^2 - 0.015290486789618418\eta^4$$

$$0.005908636179836585\eta^5 - 0.0007217813686457765\eta^6$$

$$-0.0001242241428572202\eta^7 + 0.00002275370057978931 4\eta^8 + \ldots\ldots\ldots \quad (20)$$

To corroborate the current result of the problem and endorse accurateness, the VIM results are benchmarked with an alternative (numerical) method. Numerical solutions are obtained with quadrature in the symbolic code, MATLAB. An excellent agreement is achieved between the present VIM technique and numerical solutions for the case of $M = 1.0, \alpha = 1.0, \beta = 0.2, \xi = 1.0$ as shown in **Table 1**. Further validation of the VIM solutions is attained by comparing the VIM in Fig. 2 with the earlier of Nadeem *et al.* [52] for Newtonian hydromagnetic shrinking sheet flow i.e., neglecting couple stresses ($\xi = 0$). Furthermore, the present VIM solution is also compared graphically in Fig. 3 with the previous results of Fang *et al.* [46] *for non-magnetic*

*Newtonian shrinking sheet flow* when $\xi = 0, M = 0$. Again, excellent correlation is achieved which endorses the validity of the VIM computations. Confidence in the VIM code is therefore justifiably high.

| $\eta$ | $f(\eta)$ | | |
|---|---|---|---|
| | VIM | Numerical | Error |
| 0 | 1.0 | 1.0 | 0.0 |
| 0.1 | 0.968487 | 0.969699 | 0.00045 |
| 0.2 | 0.937421 | 0.939413 | 0.00018 |
| 0.3 | 0.906147 | 0.909155 | 0.00024 |
| 0.4 | 0.869834 | 0.878937 | 0.00014 |
| 0.5 | 0.838671 | 0.848774 | 0.00012 |
| 0.6 | 0.808668 | 0.818677 | 0.00071 |
| 0.7 | 0.778143 | 0.788657 | 0.00033 |
| 0.8 | 0.738425 | 0.758724 | 0.00060 |
| 0.9 | 0.708791 | 0.728890 | 0.00067 |
| 1.0 | 0.689267 | 0.699166 | 0.00087 |

**Table 1:** VIM and numerical solution comparison for $M = 1.0, \alpha = 1.0, \beta = 0.2, \xi = 1.0$

## 4. RESULTS AND DISCUSSION

The effects of several evolving flow-field parameters namely wall transpiration parameter ($\alpha$), unsteadiness parameter ($\beta$), couple stress parameter ($\xi$) and magnetic body force number ($M$) on velocity $f'(\eta)$ profiles are visualized graphically to provide an insight into the physics of the flow problem.

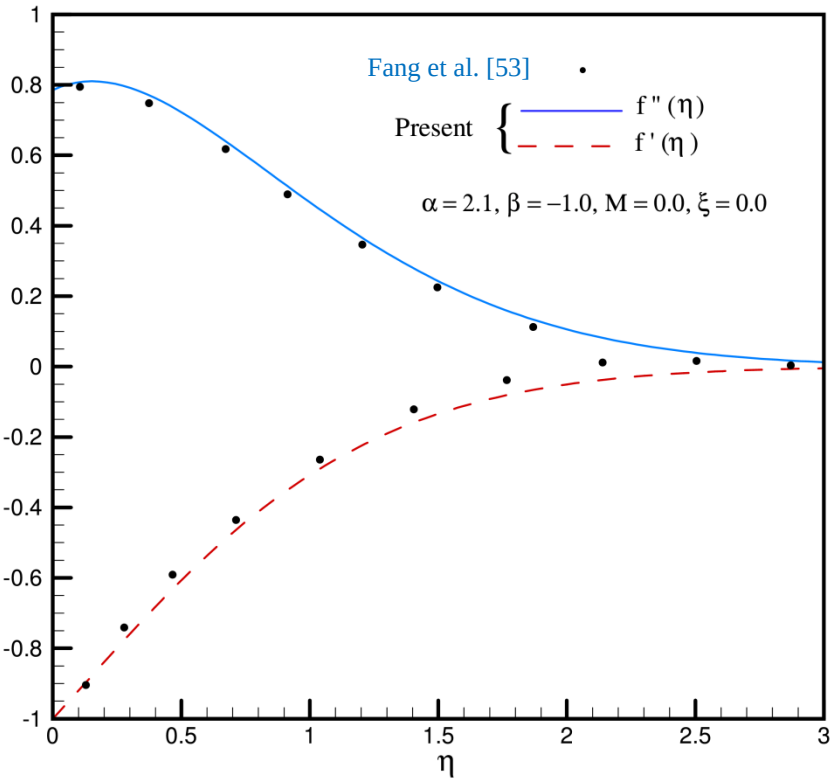


**Fig. 2:** Comparison of flow field profiles with Fang *et al.* [53] when $M = 0, \xi = 0$.

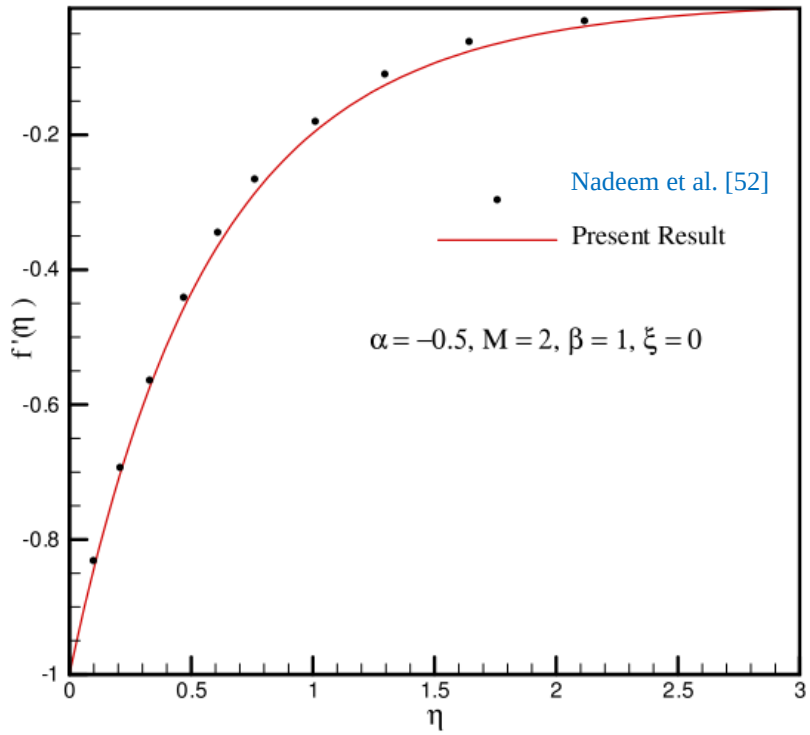


**Fig. 3:** Comparison of flow field profiles with Nadeem *et al.* [52] when $\xi = 0$.

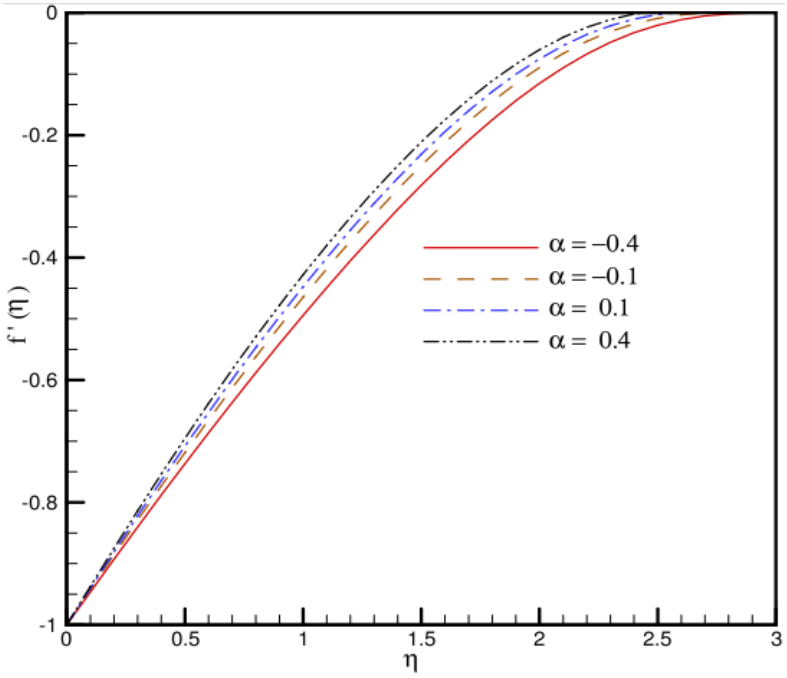


**Fig. 4:** Velocity profile for various values of $\alpha$ when $M = 1, \xi = 1, \beta = 1$.

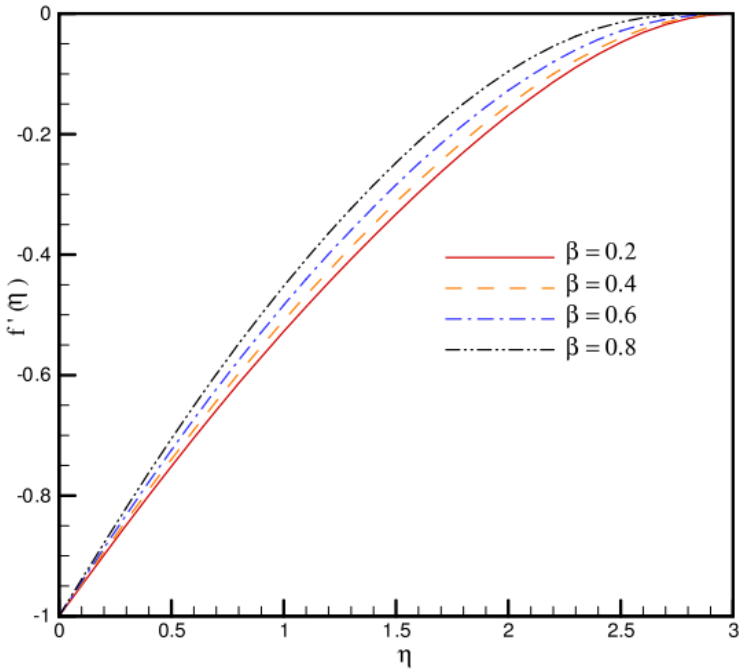


**Fig. 5:** Velocity profile for various values of β when $M = 1, \xi = 1, \alpha = 1$.

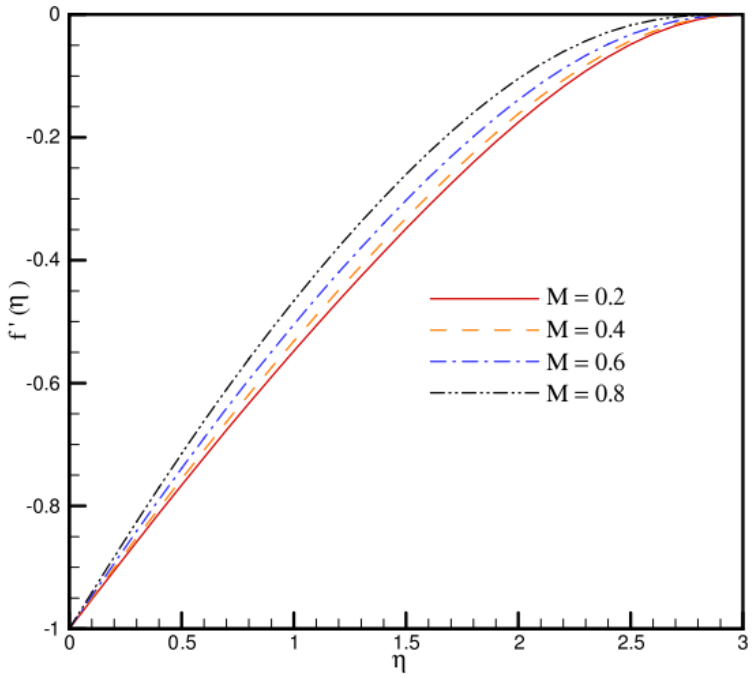


**Fig. 6:** Velocity profile for various values of β when $M = 1, \xi = 1, \alpha = 1$.

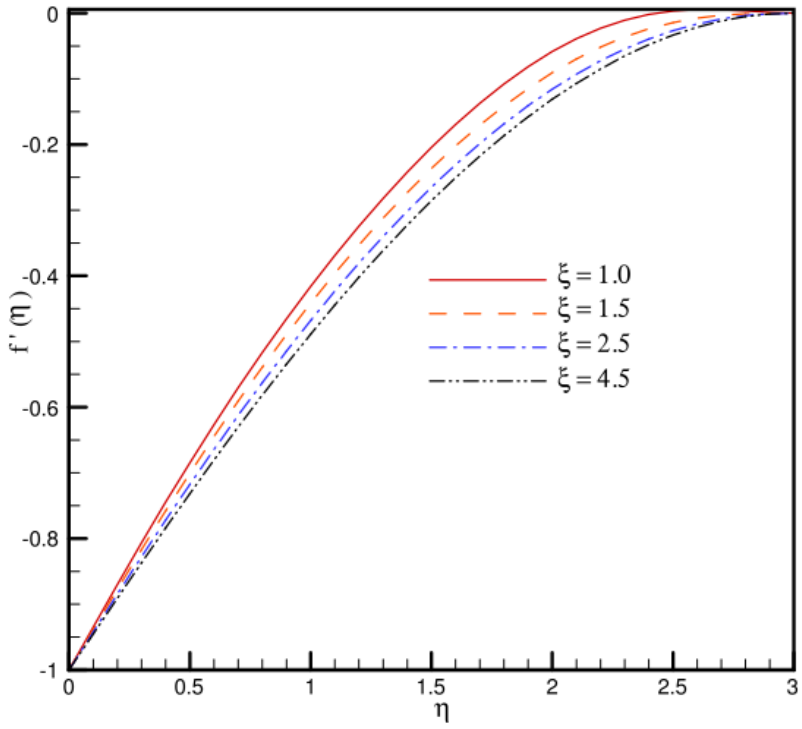


**Fig. 7:** Velocity profile for various values of $\xi$ when $M = 1, \beta = 1, \alpha = 1$.

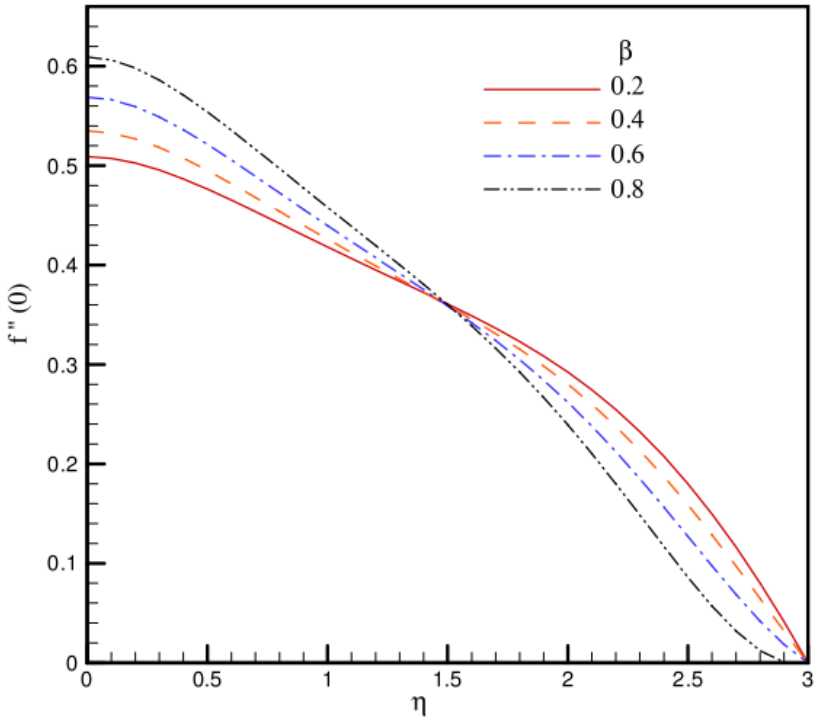


**Fig. 8:** Velocity profile for various values of β when $M = 1, \xi = 1, \alpha = 1$.

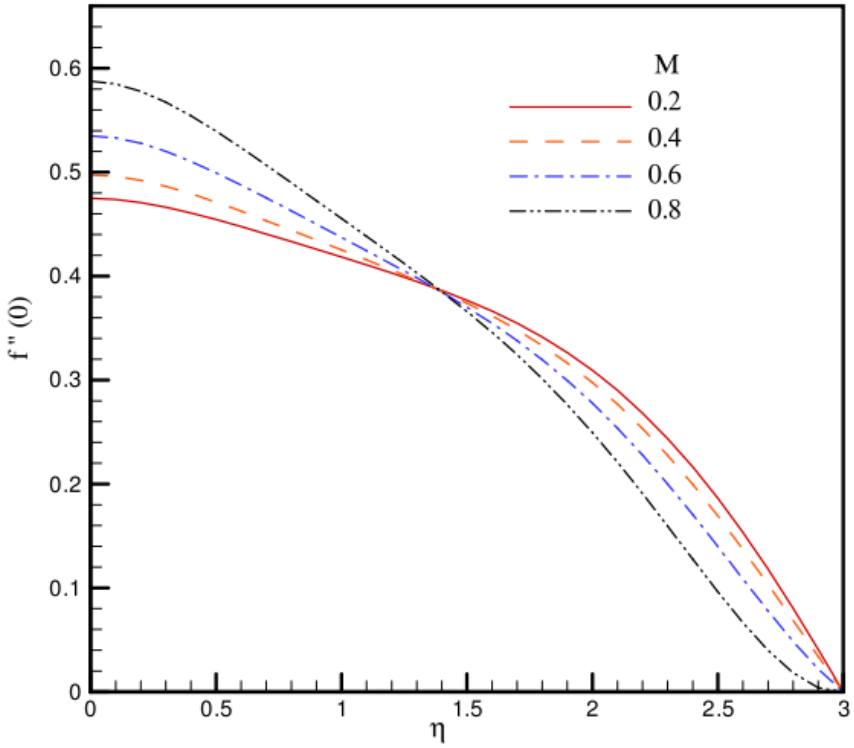


**Fig. 9:** Velocity profile for various values of $M$ when $\beta = 1, \xi = 1, \alpha = 1$.

**Fig. 4** depicts the impact of wall transpiration parameter, $\alpha$ for both suction ($\alpha > 0$) and injection ($\alpha < 0$) cases on velocity evolution, $f'(\eta)$. It is noticed from Fig. 4 that an augmentation in positive values of $\alpha$ the velocity increases and consequently the thickness of the momentum (hydrodynamic) boundary layer decreases. This is the opposite behavior to that associated with a stretching sheet in which suction ($\alpha > 0$) induces a decrease in velocity by causing adhesion of the momentum boundary layer to the wall. For the *shrinking* sheet, suction generates acceleration and thinning of the momentum boundary layer, as noted in a number of previous investigations including Prasad *et al*. [8] and Hafidzuddin *et al*. [9]. The polymer therefore shears faster at the wall with suction. However, injection clearly induces deceleration and suppresses velocity magnitudes. It is also of note that negative velocities are computed at all values of the transverse coordinate, $\eta$, and this is also characteristic of shrinking (contracting) sheet behavior in rheological liquids, as elaborated in detail by Gupta *et al.* [23] and also Latiff *et al*. [26]. This may also be associated with tensile stresses in the non-Newtonian fluid which are influenced differently when the sheet is shrinking compared to extending (stretching), as described by Kistler and Schweizer [2]. Evidently the porous nature of the wall exerts a substantial and non-trivial influence on momentum diffusion rate and noticeably modifies boundary layer thickness.

**Fig. 5** examines the effects of the unsteadiness parameter $\beta$ on velocity profile. Although transient terms are not incorporated in the primitive momentum boundary layer eqn. (2), it is simulated via the parameter, $\beta$, which itself is a function of the original unsteadiness parameter, $a$. The latter features in the shrinking velocity and transpiration velocity as well as the unsteady magnetic field term, as defined in Eqns. (4a, b). Increasing $\beta$ values imply increasingly unsteady shrinking at the wall and this serves to accelerate the flow by boosting momentum diffusion in the boundary layer. The momentum boundary layer is therefore reduced in thickness. The unsteadiness term, $+\frac{1}{2}\beta\eta f''$ in the transformed momentum Eqn. (6) is clearly a *positive* term and this assists the momentum development leading to flow acceleration. The steady-state case is retrieved for $\beta \to 0$, which is unrealistic for real polymer processing flows where transient conditions are frequently encountered [1, 2]. The negative velocity values imply that motion is in the opposite direction to the positive *x*-coordinate (Fig. 1), since the sheet is contracting.

**Fig. 6** depicts the influence of magnetic body force parameter, *M*, on velocity distribution. This parameter is different from the classical Hartmann number featuring in MHD simulations which

relates *magnetic body force to viscous hydrodynamic force*. The parameter, $M^2 = \sigma B_0^2/\rho U_0(1-at)$ effectively relates the Lorentz magnetic body force to the inertial force (momentum force) in the flow. Varying *M* does not induce the same effect on the velocity field as would the classical Hartmann number since the current regime is shrinking and is not a conventional fluid dynamic scenario (e.g. flow past a flat plate). Higher *M* values are observed to increase velocity i.e. accelerate the flow. This is the converse effect to conventional magnetohydrodynamic viscous flow from a flat plate in which stronger magnetic field is known to induce damping in the flow (deceleration). Increasing the Lorentz body force therefore acts in a similar fashion to the magnetic field moving with the free stream and this results in acceleration in the flow and a reduction in momentum boundary layer thickness. The magnetic force term is assistive to the flow as observed in Eqn. (6), viz, $+(M^2+\beta)f'$ and this manifests in a boost in the flow with stronger magnetic field. This effect has been confirmed by several researchers including Thumma *et al.* [37], Zheng *et al.* [41] and Uddin *et al.* [43] and is associated with shrinking sheets. At the wall ($\eta$=0), the no-slip boundary condition is enforced in Eqn. (7) i.e. $f'(\eta) \to 0$. No velocity overshoot is observed as with stretching sheet flows [43]. It is also noteworthy that velocity values again are always negative at all values of *M* indicating that there is no flow reversal (backflow) in the boundary layer irrespective of the strength of the magnetic field. Overall the magnetic field exerts a significant control effect on momentum characteristics and is therefore a simple but elegant excellent mechanism for regulating manufacturing flows.

**Fig. 7** illustrates the impact of the rheological couple stress fluid parameter, $\xi$, on velocity profile distribution. As $\xi$ upsurges the velocity is strongly suppressed and the momentum boundary layer thickness is markedly increased. The couple stress parameter features in the highest order derivative in the transformed momentum Eqn. (6), namely $\xi f^v$. $\xi = U_0\eta_1/\upsilon^2\rho(1-at)$ and this parameter is directly proportional to the couple stress viscosity $\eta_1$ but inversely proportional to Newtonian kinematic viscosity, $\upsilon^2$. Increasing values of this parameter will therefore imply that polar (couple stress) viscosity dominates in the magnetic polymer and will decrease momentum diffusion rate. This will lead to a decrease in the flow and a thickening in the momentum (velocity) boundary layer. Similarly, Ramesh *et al*. [30] also has got the comparable observations.

Finally, **Figs. 8-9** describe the variation of skin-friction profile ($f''(0)$) for distinct values of unsteadiness parameter, $\beta$ and magnetic body force parameter, *M*. The skin-friction graphs are

similar in both plots and both follow two distinct trends for varying values of physical parameters. As $\beta$ *and* $M$ values are increased, the skin friction $f''(0)$ exhibits an increasing trend for $0 < \eta < 1.5$ and a decreasing tendency for $\eta > 1.5$. This implies that the impact of unsteadiness and applied magnetic field are dependent on the location transverse to the sheet surface and do not impart consistent effects everywhere through the boundary layer thickness. Closer to the wall (shrinking sheet surface) stronger magnetic field and greater unsteadiness induce deceleration (decreasing skin friction) whereas further from the wall towards the free stream both parameters increasing result in significant flow acceleration.

## 5. CONCLUSIONS

In the present article, a mathematical model has been established for magnetohydrodynamic flow of an electrically conducting non-Newtonian couple stress fluid from a transient shrinking (contracting) porous sheet. Suction/injection effects at the wall have been considered and also unsteady magnetic field and linear shrinking of the sheet. The transformed momentum boundary layer equation has been solved under appropriate boundary conditions with a variational iteration method (VIM) which is a semi-analytical/numerical scheme employing Lagrangian multipliers. The study to validate the current results has been conducted with previous Newtonian hydromagnetic and non-magnetic studies. Further verification of the general model with MATLAB numerical quadrature has also been included. The general boundary value problem has been shown to be dictated by four parameters- couple stress (rheological), unsteadiness, magnetic body force parameter, wall transpiration (suction/injection) parameters. The outcomes of the current study have shown that:

(i) Increasing magnetic field (higher magnetic number) generates flow acceleration and decreases momentum boundary layer thickness.

(ii) Increasing suction (lateral mass flux removal) at the wall produces strong acceleration in the flow whereas increasing injection (lateral mass flux blowing) produces deceleration and a thicker momentum boundary layer.

(iii) Increasing unsteadiness parameter induces strong acceleration is induced with higher unsteadiness parameter values. due to the shrinking sheet dynamics.

(iv) Increasing rheological (couple stress) parameter results in a strong retardation in the boundary layer flow and a growth in momentum (hydrodynamic) boundary layer thickness.

(v) Increasing unsteadiness and magnetic body force parameter induce retardation closer to the wall (shrinking sheet surface) whereas further from the wall (in the transverse direction) towards the free stream both parameters increasing results in a marked flow acceleration.

(vi) VIM demonstrates excellent convergence and accuracy and shows significant promise in studying further magnetic polymer fabrication flow problems.

The present computations may be extended to consider more advanced microstructural non-Newtonian models e.g. Eringen's micropolar model [55] and also slip effects [56]. These aspects are currently under investigation.

**REFERENCES**

[1] A. Torres *et al.* "Properties predictor for HDPE/LDPE/LLDPE blends for shrink film applications". *Journal of Plastic Film and Sheeting*, 22 (1), pp.29-37 (2006).

[2] Kistler, SF, Schweizer, PM. *Liquid Film Coating: Scientific Principles and Their Technological Implications*. Chapman & Hall, New York, USA (1997).

[3] Wang, C. Y., "Liquid film on an unsteady stretching sheet", *Quart. Appl. Math*., 48, pp. 601-610 (1990).

[4] Miklavcˇicˇ M, Wang CY, Viscous flow due to a shrinking sheet. *Quart. Appl. Math*. 64: 283–290 (2006).

[5] T. Fang, "Boundary layer flow over a shrinking sheet with power-law velocity", *International Journal of Heat and Mass Transfer* 51, 5838–5843 (2008).

[6] T.Fang, W. Liang, C. F. Lee, "A new solution branch for the Blasius equation—A shrinking sheet problem", *Computers and Mathematics with Applications* 56, 3088–3095 (2008).

[7] F. M. Ali, R. Nazar, N. M. Arifin and I. Pop, "Unsteady shrinking sheet with mass transfer in a rotating fluid", *Int. J. Numer. Meth. Fluids*, 66:1465–1474 (2011).

[8] K. V. Prasad, K. Vajravelu and I. Pop, "Flow and heat transfer at a nonlinearly shrinking porous sheet: the case of asymptotically large power law shrinking rates", *Int. J. of Applied Mechanics and Engineering*, 18, No.3, pp.779-791 (2013).

[9] M. E. H. Hafidzuddin, R. Nazar, N. M. Arifin and I. Pop, "Three-dimensional viscous flow and heat transfer over a permeable shrinking sheet", *International Communications in Heat and Mass Transfer*, 56, 109-113 (2014).

[10] S. Ghosh, S. Mukhopadhyay, and K. Vajravelu, "Dual solutions of slip flow past a nonlinearly shrinking permeable sheet", *Alexandria Engineering Journal*, 55, 1835-1840 (2016).

[11] Md. S. Uddin and K. Bhattacharyya, "Thermal boundary layer in stagnation-point flow past a permeable shrinking sheet with variable surface temperature", Propulsion and Power Research, 6, 186-194 (2017).

[12] C.D. Han, *Rheology in Polymer Processing*, Academic Press, Orlando, USA (1976).

[13] H. Sobhani *et al.*, "Non-isothermal modeling of a non-Newtonian fluid flow in a twin-screw extruder using the fictitious domain method", *Macromolecular Theory and Simulations*, 22, 462-474 (2013).

[14] A. Romo-Uribe, "Dynamics and viscoelastic behavior of waterborne acrylic polymer/silica nanocomposite coatings", *Progress in Organic Coatings*, 129, 125-132 (2019).

[15] A. Zaib *et al*., "Dual solutions of non-Newtonian Casson fluid flow and heat transfer over an exponentially permeable shrinking sheet with viscous dissipation", Modelling and Simulation in Engineering, Volume 2016, Article ID 6968371, 8 pages http://dx.doi.org/10.1155/2016/6968371

[16] R. Mehmood, Rabil Tabassum, S. Kuharat, O. Anwar Bég and M. Babaie, "Thermal slip in oblique radiative nano-polymer gel transport with temperature-dependent viscosity: solar collector nanomaterial coating manufacturing simulation", *Arabian J. Science and Engineering* (2018). *https://doi.org/10.1007/s13369-018-3599-y (17 pages)*

[17] Ishak, A., Lok, Y. Y. and Pop, I. “Non-Newtonian power-law fluid flow past a shrinking sheet with suction”. *Chemical Engineering Communications*, 199(1), 142-150 (2011).

[18] Fang, T.-G., Tao, H., & Zhong, Y.-F. “Non-Newtonian power-law fluid flow over a shrinking sheet”. *Chinese Physics Letters*, 29(11), 114703-6 (2012).

[19] A. Ishak, Y. Y. Lok, and I. Pop, “Stagnation-point flow over a shrinking sheet in a micropolar fluid,” *Chemical Engineering Communications*, vol. 197, no. 11, pp. 1417–1427, (2010).

[20] N. C. Roşca, I. Pop, “Boundary layer flow past a permeable shrinking sheet in a micropolar fluid with a second order slip flow model”, *European Journal of Mechanics B/Fluids* 48, 115-122 (2014).

[21] Zaib, A., Bhattacharyya, K., Uddin, M. S., & Shafie, S., “Dual solutions of non-Newtonian Casson fluid flow and heat transfer over an exponentially permeable shrinking sheet with viscous dissipation”. *Modelling and Simulation in Engineering*, 2016, 1-8 (2016).

[22] Naganthran, K., Nazar, R., and Pop, I. “Stability analysis of impinging oblique stagnation-point flow over a permeable shrinking surface in a viscoelastic fluid*”. International Journal of Mechanical Sciences*, 131-132, 663-671 (2017).

[23] D. Gupta, Lokendra Kumar, O. Anwar Bég and B.Singh, “Finite element simulation of mixed convection flow of micropolar fluid over a shrinking sheet with thermal radiation”, *Proc IMechE-Part E: J. Process Mechanical Engineering,* 228 (1) 61-72 (2014).

[24] Mishra, S. R., Khan, I., Al-mdallal Q.M., & Asifa, “T. Free convective micropolar fluid flow and heat transfer over a shrinking sheet with heat source”. *Case Studies in Thermal Engineering,* 11, 113-119 (2018).

[25] Khan, M., Sardar, H., Gulzar, M. M., & Alshomrani, A. S. “ On multiple solutions of non-Newtonian Carreau fluid flow over an inclined shrinking sheet”. Results in Physics, 8, 926–932 (2018).

[26] N.A. Latiff, M. J. Uddin, O. Anwar Bég and A.I.M. Ismail, “Unsteady forced bioconvection slip flow of a micropolar nanofluid from a stretching/ shrinking sheet”, *Proc. IMechE- Part N: J. Nanoengineering and Nanosystems,* 230 (4) pp. 177–187 (2016).

[27] V. K. Stokes, Couple stresses in fluids, *Physics of Fluids*, 9, pp. 1709-1715 (1966).

[28] V.K. Stokes, *Theories of fluids with microstructures*, Springer, New York (1984).

[29] D. Tripathi, A. Yadav and O. Anwar Bég, "Electro-osmotic flow of couple stress fluids in a micro-channel propagated by peristalsis", *European Physical Journal Plus,* 132: 173-185. (2017).

[30] K. Ramesh, D. Tripathi, O. Anwar Bég, "Cilia-assisted hydromagnetic pumping of biorheological couple stress fluids", *Propulsion and Power Research* (2019). *https://doi.org/10.1016/j.jppr.2018.06.002* (13 pages)

[31] H. Basha, G. Janardhana Reddy, N. S. Venkata Narayanan and O. Anwar Bég, "Supercritical heat transfer characteristics of couple stress convection flow from a vertical cylinder using an equation of state approach", *J. Molecular Liquids (2018).* (20 pages) *doi.org/10.1016/j.molliq.2018.11.165*

[32] H. J Schneider-Muntau and H. Wada (Eds)., "Materials Processing in Magnetic Fields", *Proceedings of the International Workshop on Materials Analysis and Processing in Magnetic Fields, Tallahassee, Florida, USA, 17 – 19 March* (2004).

[33] G. Longo *et al.,* "Morphological characterization of innovative electroconductive polymers in early stages of growth", *Surface and Coatings Technology,* 207, 286-292 (2012).

[34] J. Thévenot, "Magnetic responsive polymer composite materials", *Chem. Soc. Rev.*, 42, 7099-7116 (2013).

[35] K. Pavlov, "Magnetohydrodynamic flow of an incompressible viscous fluid caused by deformation of a plane surface", *Magnitnaya Gidrodinamika,* 4 (1974), pp. 146-147.

[36] O. Anwar Bég, S. Kuharat, M. Ferdows, M. Das, A. Kadir, M. Shamshuddin, "Magnetic nano-polymer flow with magnetic induction and nanoparticle solid volume fraction effects: solar magnetic nano-polymer fabrication simulation*", Proc. IMechE-Part N: J Nanoengineering, Nanomaterials and Nano-systems (2019).* DOI: 10.1177/ 2397791419838714 (19 pages)

[37] T. Thumma, O. Anwar Bég and A. Kadir, "Numerical study of heat source/sink effects on dissipative magnetic nanofluid flow from a non-linear inclined stretching/shrinking sheet", *J. Molecular Liquids,* 232, 159-173 (2017).

[38] R. Cortell, "On a certain boundary value problem arising in shrinking sheet flows", *Applied Mathematics and Computation*, 217, 4086-4093 (2010).

[39] N.F.M. Noor, S. A. Kechil, and I. Hashim, "Simple non-perturbative solution for MHD viscous flow due to a shrinking sheet", *Commun Nonlinear Sci Num Simul.,* 15, 144-148 (2010).

[40] J.H. Merkin, V. Kumaran, "The unsteady MHD boundary-layer flow on a shrinking sheet", *European Journal of Mechanics B/Fluids,* 29, 357-363 (2010).

[41] L. Zheng, J. Niu, X. Zhang, Y. Gao, "MHD flow and heat transfer over a porous shrinking surface with velocity slip and temperature jump", *Mathematical and Computer Modelling*, 56, 133-144 (2012).

[42] T. Hayat, Z. Abbas and M. Sajid, "On the analytic solution of magnetohydrodynamic flow of a second-grade fluid over a shrinking sheet", *ASME Journal of Applied Mechanics,* 74, 1165-71 (2007).

[43] M.J. Uddin, O. Anwar Bég and N.S. Amin, "Hydromagnetic transport phenomena from a stretching or shrinking nonlinear nanomaterial sheet with Navier slip and convective heating: a model for bio-nano-materials processing", *J. Magnetism Magnetic Materials,* 368, 252-261(2014).

[44] J. H. He, "Variational iteration method-a kind of non-linear analytical technique: some examples," *International Journal of Non-Linear Mechanics,* vol. 34, no. 4, pp. 699–708 (1999).

[45] B. Batiha, M.S.M. Noorani, I. Hashim, "Variational iteration method for solving multispecies Lotka–Volterra equations" *Computers and Mathematics with Applications* 54 903-909 (2007).

[46] L. Xu and E. W. M. Lee, "Variational Iteration Method for the magnetohydrodynamic flow over a nonlinear stretching sheet", *Abstract and Applied Analysis,* 2013, Article ID 573782, 1-5 (2013).

[47] B. Eerdun , Q. Eerdun , B. Huhe , C. Temuer , J. Y. Wang, "Variational iteration method with He's polynomials for MHD Falkner-Skan flow over permeable wall based on Lie symmetry method", *International Journal of Numerical Methods for Heat & Fluid Flow*, 24, pp. 1348-1362 (2014).

[48] M. Moosavi, M. Momeni, T. Tavangar, R. Mohammadyari and M. Rahimi-Esbo, "Variational iteration method for flow of non-Newtonian fluid on a moving belt and in a collector", *Alexandria Engineering Journal*, 55, 1775-1783 (2016).

[49] O. Anwar Bég, S.S. Motsa, M.N. Islam and M. Lockwood, "Pseudo-spectral and variational iteration simulation of exothermically reacting Rivlin-Ericksen viscoelastic flow and heat transfer in a rocket propulsion duct", *Computational Thermal Sciences*, 6, 2, 91-102 (2014).

[50] Assma F. Elsayed and O. Anwar Bég, "New computational approaches for biophysical heat transfer in tissue under ultrasonic waves: Variational iteration and Chebyschev spectral simulations", *J. Mechanics Medicine Biology, 14, 3, 1450043.1-1450043.17 (17 pages) (2014).*

[51] O. Anwar Bég, "Numerical methods for multi-physical magnetohydrodynamics", Chapter 1, pp. 1-112, *New Developments in Hydrodynamics Research, M. J. Ibragimov and M. A. Anisimov, Eds., Nova Science, New York, September* (2012).

[52] S. Nadeem, R. Ul Haq and C. Lee "MHD boundary layer flow over an unsteady shrinking sheet: analytical and numerical approach", *J Braz. Soc. Mech. Sci. Eng*. 37, 1339-1346 (2015).

[53] T. G. Fang, J. Zhang and S. S. Yao, "Viscous flow over an unsteady shrinking sheet with mass transfer", *Chin. Phys. Lett*. 26, 014703-5 (2009).

[54] *MATHEMATICA Handbook*, Wolfram Research, USA (2019).

[55] D. Gupta, Lokendra Kumar, O. Anwar Bég and B. Singh, "Finite element analysis of MHD flow of micropolar fluid over a shrinking sheet with a convective surface boundary condition", *J. Engineering Thermophysics*, 27, 202–220 (2018).

[56] M.J. Uddin, O. Anwar Bég and A.I. Ismail, Radiative-convective nanofluid flow past a stretching/shrinking sheet with slip effects, *AIAA J. Thermophysics Heat Transfer*, 29, 3, 513-523 (2015).